Japanese Journal of Applied Physics
Vol. 46, No. 6A, 2007, pp. 3560–3565

©2007 The Japan Society of Applied Physics

Transport Coefficients for Electrons in Mixtures of Ar and HBr

Olivera ŠAŠIĆ*, Saša DUJKO, Zoran Lj. PETROVIĆ†, and Toshiaki MAKABE[1]

Institute of Physics, PO Box 68, 11080 Zemun, Belgrade, Serbia
[1]*Department of Electrical Engineering, Keio University, 3-14-1 Hiyoshi, Kohoku-ku, Yokohama 223-8522, Japan*

(Received February 28, 2006; accepted February 23, 2007; published online June 6, 2007)

We present calculations of swarm data and rate coefficients for electrons in mixtures of Ar and HBr. The transport data were calculated using a Monte Carlo simulation over a broad range of E/N (electric field E to the gas number density N ratio) and with the idea to provide a basis for models of plasma etching involving HBr. The total cross section has an almost a constant collision frequency, which leads to rather uneventful E/N dependences of the transport data in pure HBr, but the mixtures with Ar involve more complex kinetic phenomena. [DOI: 10.1143/JJAP.46.3560]

KEYWORDS: HBr, transport coefficients, electron transport, collisions, swarms, fluid models, plasma etching

1. Introduction

HBr has an important role in the plasma processing of ICs. It has been used for numerous processes[1–3] such as the etching of poly Si,[4,5] III–V semiconductors,[6] heterostructures,[7] HfO_2 (which is used as a high-k gate oxide), and organo-silicate glasses (e.g., black diamond, which is used as a low-k oxide for interconnects).[8] The functionality of HBr in plasma etching is achieved in various mixtures. Usually it is combined with Br_2, Cl_2,[4] or SF_6–O_2,[9] but it has been also used with $SiCl_4$–SiF_4,[10] BCl_3, CH_4,[11] H_2, and even as a pure gas.[6] It was shown that an etching rate of 11 nm/min for III–V semiconductor etching could be achieved in mixtures of HBr with argon.[12] Thus one can see that HBr has suitable properties[13,14] for a number of applications, such as a fast etching rate, high selectivity[4,10,15] and a high degree of anisotropy with the ability to produce very-high-aspect-ratio[9] structures in the substrate. Thus, it is surprising that there are no detailed models of HBr-containing plasmas to our knowledge. In the few cases when models were developed for etching using HBr containing mixtures, the plasma was assumed to have the same properties as Cl_2 plasma and only the properties of the ions were changed to take into account the difference in mass.[16,17]

It seems that the critical problem in the development of HBr plasma models has been the shortage of data for electron HBr scattering, which is the first step that provides the foundation of the description of plasmas and the lack of either cross-section or transport data (or both) makes it impossible to provide an accurate description of collisional plasmas. However, in recent years HBr has attracted interest from the community of scientists dealing with electron-molecule collisions. As a polar molecule, HBr has very large cross sections at small energies and a strong resonant vibrational excitation. Comprehensive studies have been carried out covering mainly the vibrational excitation and momentum transfer. Good agreements have been achieved between different sources of data, most importantly, between theoretical and experimental data.

For the calculation of transport data and for plasma modeling, it is necessary to have a complete set of cross sections (i.e., a set representing energy and momentum balance). Thus, if a process is missing from the set, regardless of how accurate other the cross sections are, the results may be far from accurate. We have compiled a set of cross sections for HBr and we have also made the necessary extrapolations to achieve a reasonably complete set[18–20] that is based primarily on the available theoretical and experimental data.

In this paper, we present calculations of the transport coefficients and rates of inelastic processes in a 5% HBr–95% Ar mixture. The data may prove to be a basis for modeling such mixtures,[6,12] but, more importantly, it will reveal the basic characteristics of the transport data and may encourage the experimental measurements necessary to improve the uniqueness and reliability of the set of cross section data. The calculations were made for DC fields and also for $E \times B$ DC and RF fields.

1.1 Cross section data

We have compiled a set of the most accurate, available, cross sections from the literature for electron scattering on HBr. In particular, a good data are available for vibrational excitation and dissociative attachment in the recent results of groups of Horáček and Allan.[21] Sparse results for momentum transfer or total elastic scattering[22] had to be extrapolated. From 0.5 eV to the zero energy we used the shape of the cross section for HCl to provide the energy dependence, while the magnitude was adjusted to fit the data for HBr. Beyond 10 eV we used the Born approximation to extend data to higher energies. The data for ionization cross section were not available in the literature, and they were kindly calculated for us by Kim.[23] The excitation cross sections of Rescigno[22] were used, but they had to be augmented by an estimate of the total excitation (including dissociation to the ground state) cross section, which was based on the data for HCl.[24] The cross section set for HBr is sufficiently complete and accurate to calculate the transport data for pure gas and, in particular, for mixtures of rare gases and HBr. Thus, it may be used as a part of the database for the modeling of processing plasmas.[18,19]

Since there are no detailed measurements of swarm data, the cross sections could not be validated by a swarm procedure. However, measurements of the cross sections were made and the results are in excellent agreement with the calculated cross sections. We have shown the set of cross sections for electrons in pure HBr in Fig. 1.

*Also at Faculty of Traffic Engineering, University of Belgrade.
†Also at Serbian Academy of Sciences and Arts, Belgrade, Serbia.
E-mail address: zoran@phy.bg.ac.yu

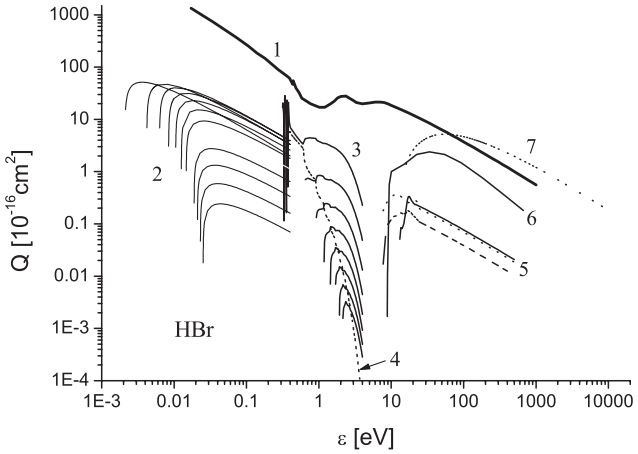

Fig. 1. Cross sections for electrons in HBr. Cross sections in the figure are: 1 — elastic momentum transfer; 2 — rotational excitation cross sections; 3 — vibrational excitation cross sections; 4 — electron attachment; 5 — electronic excitation cross sections; 6 — effective dissociation cross section and 7 — ionization cross section.

The special characteristics of the set of cross sections are that the magnitude of the momentum transfer cross section is extremely high and that, as for most polar molecules, the cross section is reduced with energy so that it is close to the constant collision frequency cross section.[18,19,22)] Vibrational cross sections are very large,[21)] with peaks of resonances of the order of 15×10^{-16} cm^2. Dissociative attachment is also very large with a peak of the order of 5×10^{-16} cm^2, which is greater than those of the most typical gases used in plasma processing by one or two orders of magnitude. These properties of the cross sections will have a decisive effect on plasma properties and, even at the abundance of 5% HBr, they will dominate both the momentum and the energy exchange in the mixture.

2. Monte Carlo Technique

The calculation of electron transport coefficients was performed using a well-tested Monte Carlo simulation code.[25,26)] The code has performed extremely well on all available dc E, dc $E \times B$, and rf $E \times B$ benchmarks. We distinguish between the real-space (bulk) and the velocity-space (flux) transport coefficients by taking into account the nonconservative nature of collisions.[27,28)] The application of transport coefficients in plasma modeling has been the subject of many studies (one recent example is ref. 29) and usually the difference between the two types of transport coefficients is not appreciated.

The definitions of the transport coefficients were given in our previous publications.[26)] However, since experimental data correspond to the bulk or real-space coefficients, we only present such data here. The drift velocities were determined from

$$W^{\mathrm{v}} = \langle v \rangle \tag{1}$$

for flux (velocity-space) drift velocities and from

$$W = \frac{d}{dt}\langle z \rangle \tag{2}$$

for bulk (real-space) drift velocities, where the electric field is directed along the z axis.

Transverse diffusion coefficients were determined from

$$ND_{\mathrm{T}} = \frac{1}{2}\frac{d}{dt}\left(\langle x^2 \rangle - \langle x \rangle^2\right) \tag{3}$$

for bulk (real-space) and from

$$ND_{\mathrm{T}}^{\mathrm{v}} = \left(\langle xV_x \rangle - \langle x \rangle \langle V_x \rangle\right) \tag{4}$$

for flux (velocity-space) diffusion coefficients. At the same time, the mobility is determined from the drift velocity and the field $\mu = W/E$. The characteristic energy eD_{T}/μ is determined from the calculated data for drift velocities and diffusion coefficients.

In addition to the rather simple scheme used in this paper, there are other ways of defining transport coefficients such as those proposed by Tagashira and coworkers,[27,30)] which also involve the definition of specific experimental systems and their conditions (see also ref. 31). Correlations between the different schemes are possible[31,32)] but are complex, and we thus chose the simple scheme that was used in our earlier papers.

Our simulations were typically performed with 5×10^5 initial electrons. The gas number density was 3.54×10^{22} m^{-3}, which corresponded to the pressure of 1 Torr (133.3 Pa) at the temperature of 273 K. The initial electron energy distribution was Maxwellian with a mean energy of 1 eV.

3. Results

3.1 DC electric field

Calculations of the basic DC transport coefficients of drift velocity and eD_{T}/μ are shown in Figs. 2 and 3, respectively. The drift velocity increases almost linearly with E/N and shows very monotonous behaviour, which is due to the energy dependence of the momentum transfer.

The characteristic energy eD_{T}/μ shows a rapid increase between 1 and 10 Td, where it was difficult to achieve convergence of the calculation in a reasonable computer time. In this respect, the behaviour is similar to that in water vapour, where the combination of sharp dissociative attachment and a large vibrational cross section leads to a rapid increase in mean energy (and also characteristic energy).[33)] In pure HBr it was easier to complete simulations at low

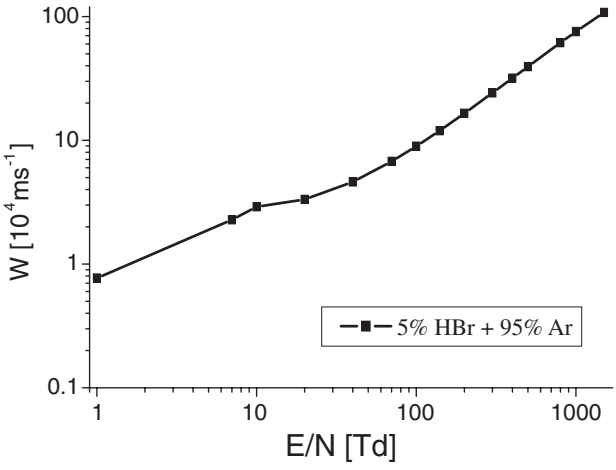

Fig. 2. Drift velocities (bulk or real-space) for electrons in 5% HBr–95% Ar mixture in DC fields. The unit for E/N is Townsend (1 Td = 10^{-21} V m^2).

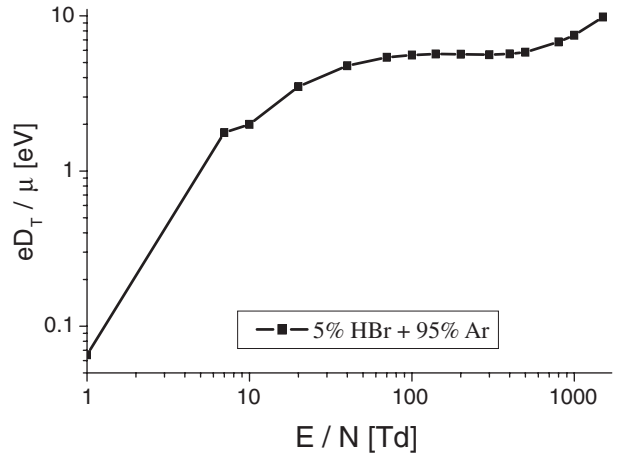

Fig. 3. eD_T/μ for electrons in 5% HBr–95% Ar mixture in DC fields.

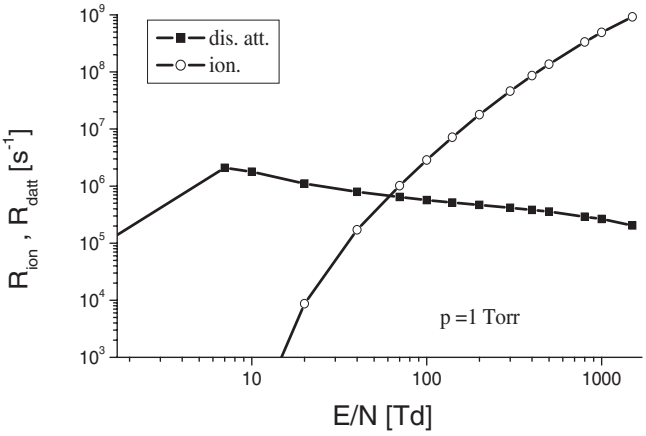

Fig. 4. Ionization and attachment rates for electrons in 5% HBr–95% Ar mixture in DC fields.

E/N. The change in eD_T/μ under these conditions is smaller, albeit it is still very rapid.

Although one may observe a large effect of the vibrational excitation of HBr on the characteristic energy eD_T/μ (the ratio of the transverse diffusion coefficient to the mobility), the effect is still sufficiently small and may be explained by a very large momentum transfer cross section in HBr. Therefore, even though the conditions are apparently favourable,[34,35] negative differential conductivity of the drift velocity in the mixture is not observed. The anisotropy of diffusion is very weak and is appreciable only between 5 and 100 Td and this can be well explained on the basis of the energy dependence of the cross sections according to the simple theory of Parker and Lowke.[26,36]

Furthermore we show the ionization and attachment rates for the mixture (Fig. 4). The condition under which ionization becomes greater than attachment is at around 60 Td. The total collision frequency is between 2×10^9 and $10 \times 10^9\ s^{-1}$, which is relevant in estimating the relaxation times necessary to apply temporal corrections in plasma models. The ionization rate becomes an appreciable part of the total collision frequency at 1000 Td.

3.2 $E \times B$ DC fields

We performed calculations for DC $E \times B$ for normalized

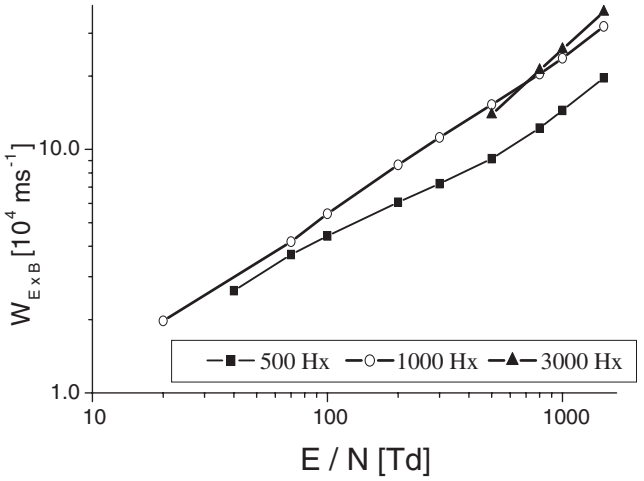

Fig. 5. Drift velocity of electrons in 5% HBr–95% Ar mixture in DC $E \times B$ fields.

magnetic fields (B/N) of 500 Hx (1 Hx $= 10^{-27}$ T m^3), 1000 Hx and 3000 Hx and for the same range for E/N. As expected, the energies are reduced with increasing B/N and the dependences of transport coefficients resemble those for the case of no magnetic field, only shifted towards a higher E/N. For all conditions covered here, the collisional frequency exceeded the cyclotron frequency. The drift velocity in the direction of the electric field does not appear to be affected by a magnetic field of less than 1000 Hx, which is a much higher limit than for other gases.[37] That is the result of the very high collisional cross sections, which maintain collision-dominated transport even for relatively high magnetic fields. The drift velocity in the $E \times B$ direction is, however, significant and peaks at around 1000 Hx (see Fig. 5). The diffusion coefficients behave in the expected manner. The $E \times B$ component very quickly becomes similar to the E component as the magnetic field increases, as predicted in the general case and in the particular case of argon.[38]

3.3 $E \times B$ RF fields

In case of Rf $E \times B$ fields with a 90° phase difference between the two fields, we performed several series of calculations as a function of E/N, B/N, and frequency. In all cases, the given values of the fields refer to peak values. Calculations were performed for 1 Torr (133 Pa according to ω/N scaling, 100 MHz corresponds to a discharge at 10 MHz and 100 mTorr, which is typical for many applications). In Fig. 6 we show drift velocities for the case when there is no magnetic field. Becouse of uneventful energy dependence of the momentum transfer cross section, the drift velocities have an almost sinusoidal shape with almost the same peak value. The only difference is the phase delay, which appears to be small until the frequency exceeds 100 MHz. This is different from the behaviour of the mean energy, where undulated mean energies are significantly delayed in phase, even for 10 MHz and for 500 MHz the phase difference is $\pi/2$, the modulation is almost lost and the mean value of the mean energy decreases with frequency.

In Figs. 7 and 8 we show the longitudinal (E) and $E \times B$ components of the drift velocity, respectively in crossed

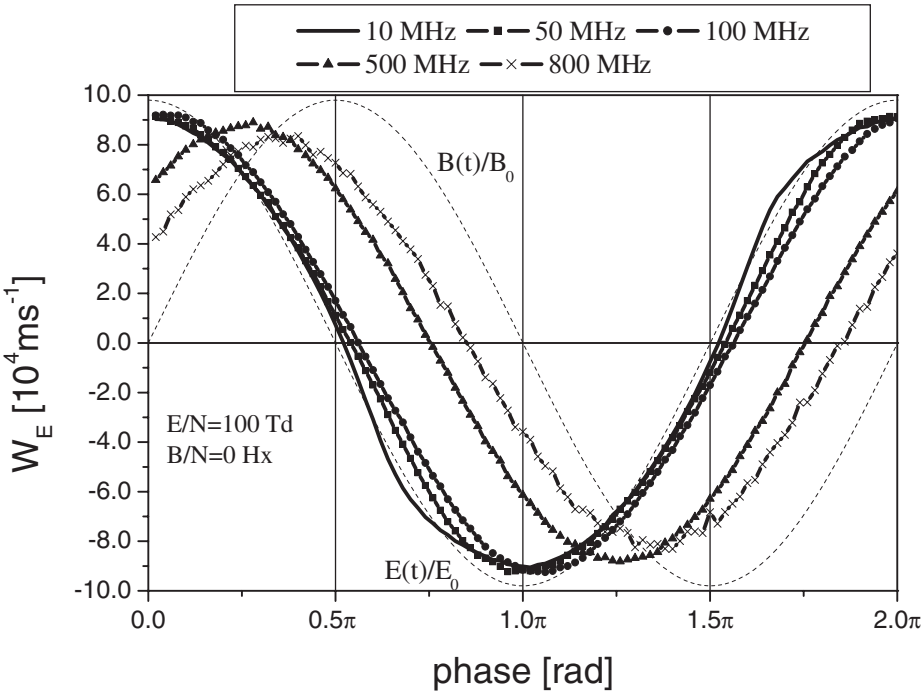

Fig. 6. Drift velocity of electrons in 5% HBr–95% Ar mixture in RF $E(t)$ field at different frequencies for $E/N = 100$ Td.

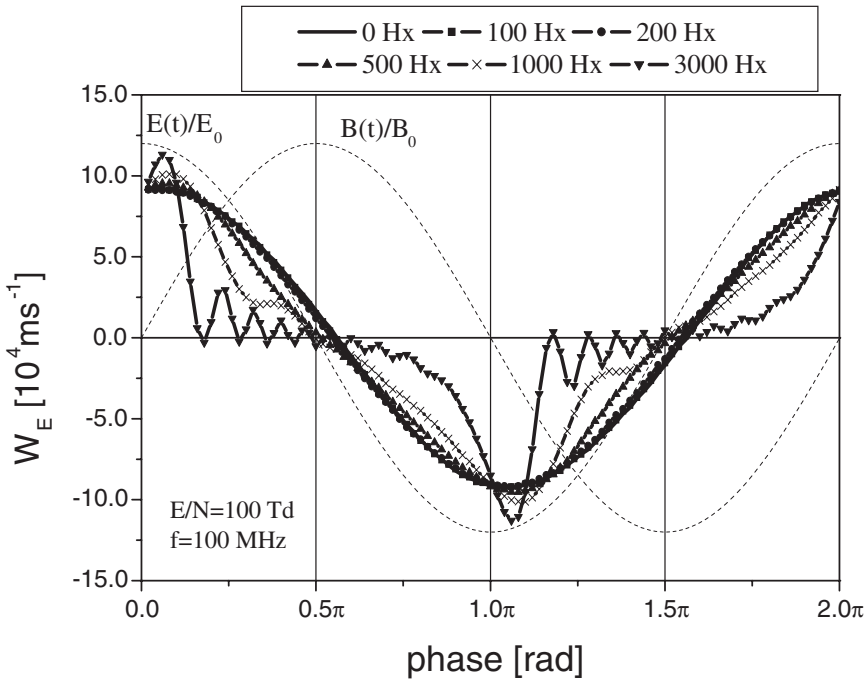

Fig. 7. Longitudinal drift velocity (W_E) of electrons in 5% HBr–95% Ar mixture in RF $E(t) \times B(t)$ field at different magnetic fields for $E/N = 100$ Td.

electric and magnetic fields as a function of time during one period and for different magnitudes of the magnetic field. For the longitudinal component, one can see that the sinusoidal shape is maintained even for very high magnetic fields, and only at 500 Hx thus some departure become visible. At the highest B/N, the shape becomes narrower and centered around $B = 0$ with some delay, and eventually oscillations, due to the effect of cyclotron motion on the random velocity of electrons, are observed.

The $E \times B$ component of the drift velocity increases steadily with the magnetic field amplitude. As expected, it has clear asymmetry (the mean value is not zero), and starting from a sinusoidal shape, it changes to a sawtooth profile that has superimposed oscillations at the highest B/N.[39,40]

The temporal variation of the components of the diffusion tensor show the usual range of kinetic effects, such as anomalous diffusion and the corresponding anisotropy that changes with the magnetic field. However, we did not observe a transition to negative values, presumably due to

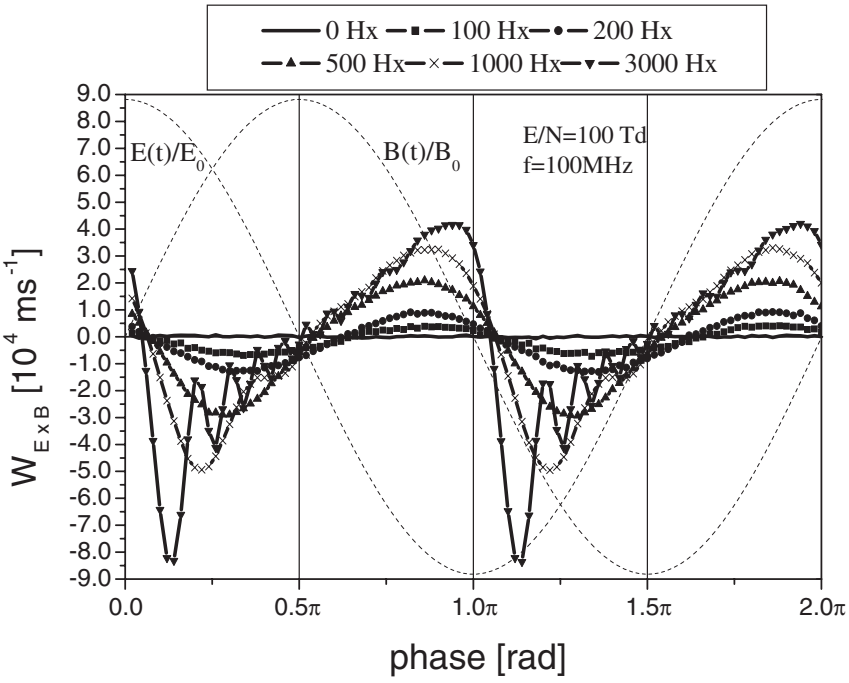

Fig. 8. Perpendicular drift velocity ($W_{E\times B}$) of electrons in 5% HBr–95% Ar mixture in RF $E(t) \times B(t)$ field at different magnetic fields for $E/N = 100$ Td.

the very strongly collisional nature of the transport obtained under the present circumstances.

4. Conclusions

The standard mixture of 5% of HBr in Ar is desirable if one wishes to increase the density of electrons in the plasma. However, the cross sections for electron scattering on HBr are so large that the dominate electron collisons and consequently transport over 20 times more abundant Ar at low energies. Thus, it seems that the strategy to use mixtures containing argon to obtain swarm data require the abundance of HBr to be very small to enable the effect of vibrational cross sections observed by measurements of the drift velocity in the mixture. At such low abundances the accuracy of preparing a mixture, particularly bearing in mind the reactive nature of HBr, may be questioned. Thus, the best strategy is still to make measurements in pure HBr and perhaps in a mixture such as the one described here. Such measurements are necessary to obtain a more accurate set of cross sections. Fortunately, becouse of the energy dependence of the cross sections, the application of fluid models for HBr is much more justified than for other standard gases.

We have produced a complete set of cross sections and transport coefficients that may be used for modeling plasmas[29] containing HBr. It requires further improvement by making measurements of the transport coefficients and ionization rates to improve accuracy. Nevertheless, the main features are the almost constant collision frequency total momentum transfer cross sections, very large vibrational excitation cross sections (considerably larger than those in nitrogen) and a very large attachment cross section, which will particularly affect the kinetics of HBr plasmas.

The present results were obtained in free spaces without any boundaries. Under plasma conditions, the coefficients obtained here should be entered into fluid or hybrid models as input data. The data and magnitude of the different effects of rf plasma kinetics may be estimated from the transport coefficients shown here. For example, data shown here may be used directly in studies of rf breakdown.[41]

Acknowledgments

Work on this paper was supported by MNTRS 141025 and by a Grant-in-Aid for the 21st century Center of Excellence Program from the Ministry of Education, Culture, Sports, Science and Technology of Japan. We thank Dr. Y. Kim, Professor J. Horáček and Professor M. Allan for providing us with their data on HBr cross sections.

1) T. D. Bestwick, G. S. Oehrlein, Y. Zhang, G. M. W. Kroesen, and E. de Fresart: Appl. Phys. Lett. **59** (1991) 336.
2) S. Xu, T. Sun, and D. Podlesnik: J. Vac. Sci. Technol. A **19** (2001) 2893.
3) L. Desvoivres, L. Vallier, and O. Joubert: J. Vac. Sci. Technol. B **19** (2001) 420.
4) K. M. Chang, T. H. Yeh, I. C. Deng, and H. C. Lin: J. Appl. Phys. **80** (1996) 3048.
5) S. A. Vitale, H. Chae, and H. H. Sawin: J. Vac. Sci. Technol. A **19** (2001) 2197.
6) S. Vicknesh and A. Ramam: J. Electrochem. Soc. **151** (2004) C772.
7) S. Agarwala, I. Adesida, C. Caneau, and R. Bhat: Appl. Phys. Lett. **62** (1993) 2830.
8) S. A. Vitale and H. H. Sawin: J. Vac. Sci. Technol. A **20** (2002) 651.
9) S. Gomez, R. Jun Belen, M. Kiehlbauch, and E. S. Aydila: J. Vac. Sci. Technol. A **23** (2005) 1592.
10) S. K. Murad, S. P. Beaumont, and C. D. W. Wilkinson: Appl. Phys. Lett. **67** (1995) 2660.
11) Y. Kuo and T. L. Tai: J. Electrochem. Soc. **145** (1998) 4313.
12) S. J. Pearton, U. K. Chakrabarti, E. Lane, A. P. Perley, C. R. Abernathy, and W. S. Hobson: J. Electrochem. Soc. **139** (1992) 856.
13) C. C. Cheng, K. V. Guinn, and V. M. Donnelly: J. Vac. Sci. Technol. B **14** (1996) 85.
14) I. Tepermeister, N. Blayo, F. P. Klemens, D. E. Ibbotson, R. A.

Gottscho, J. T. C. Lee, and H. H. Sawin: J. Vac. Sci. Technol. B **12** (1994) 2310.
15) H. Ohtake, K. Noguchi, S. Samukawa, H. Iida, A. Sato, and X. Y. Qian: J. Vac. Sci. Technol. B **18** (2000) 2495.
16) H. H. Hwang, M. Meyyappan, G. S. Mathad, and R. Ranade: J. Vac. Sci. Technol. B **20** (2002) 2199.
17) M. A. Vyvoda, M. Li, D. B. Graves, H. Lee, M. V. Malyshev, F. P. Klemens, J. T. C. Lee, and V. M. Donnelly: J. Vac. Sci. Technol. B **18** (2000) 820.
18) O. Šašić and Z. Lj. Petrović: Proc. 22nd Symp. Physics of Ionized Gases, 2004, p. 133.
19) O. Šašić and Z. Lj. Petrović: Proc. 14th Int. Symp. Electron–Molecule Collisions and Swarms, 2005, p. 84.
20) O. Šašić and Z. Lj. Petrović: submited for publication (2006).
21) M. Čižek, J. Horáček, A. Sergenton, D. Popović, M. Allan, W. Domcke, T. Leininger, and F. Gadea: Phys. Rev. A **63** (2001) 062710.
22) T. N. Rescigno: J. Chem. Phys. **104** (1996) 125.
23) Y. Kim: unpublished.
24) M. Hayashi: private communication.
25) S. Bzenić, Z. M. Raspopović, S. Sakadžić, and Z. Lj. Petrović: IEEE Trans. Plasma Sci. **27** (1999) 78.
26) Z. Lj. Petrović, Z. M. Raspopović, S. Dujko, and T. Makabe: Appl. Surf. Sci. **192** (2002) 1.
27) T. Taniguchi, H. Tagashira, and Y. Sakai: J. Phys. D **10** (1977) 2301.
28) R. E. Robson: J. Chem. Phys. **85** (1986) 4486.
29) R. E. Robson, R. D. White, and Z. Lj. Petrović: Rev. Mod. Phys. **77** (2005) 1303.
30) H. Itoh, T. Matsumura, K. Satoh, H. Date, Y. Nakao, and H. Tagashira: J. Phys. D **26** (1993) 1975.
31) R. E. Robson: Aust. J. Phys. **44** (1991) 685.
32) R. E. Robson: *Introductory Transport Theory for Charged Particles in Gases* (World Scientific, Singapore, 2006).
33) K. F. Ness and R. E. Robson: Phys. Rev. A **38** (1988) 1446.
34) Z. Lj. Petrović, R. W. Crompton, and G. N. Haddad: Aust. J. Phys. **37** (1984) 23.
35) R. E. Robson: Aust. J. Phys. **37** (1984) 35.
36) J. H. Parker and J. J. Lowke: Phys. Rev. **181** (1969) 290.
37) S. Dujko, Z. M. Raspopović, and Z. Lj. Petrović: J. Phys. D **38** (2005) 2952.
38) Z. M. Raspopović, S. Sakadžić, Z. Lj. Petrović, and T. Makabe: J. Phys. D **33** (2000) 1298.
39) Z. M. Raspopović, S. Dujko, T. Makabe, and Z. Lj. Petrović: Plasma Sources Sci. Technol. **14** (2005) 293.
40) Ž. Nikitović, O. Šašić, Z. Lj. Petrović, G. Malović, A. Strinić, S. Dujko, Z. Raspopović, and M. Radmilović-Radhenović: Mater. Sci. Forum **453–454** (2004) 15.
41) M. Radmilović-Radjenović and J. K. Lee: Phys. Plasmas **12** (2005) 063501.